# A role for the RabA4b effector protein PI-4Kβ1 in polarized expansion of root hair cells in *Arabidopsis thaliana*

Mary L. Preuss,[1] Aaron J. Schmitz,[2] Julie M. Thole,[1,3] Heather K.S. Bonner,[1] Marisa S. Otegui,[4] and Erik Nielsen[1,3]

[1]Donald Danforth Plant Science Center, St. Louis, MO 63132
[2]Department of Plant Biology, Michigan State University, East Lansing, MI 48824
[3]Department of Biology, Washington University in St. Louis, St. Louis, MO 63130
[4]Department of Botany, University of Wisconsin, Madison, WI 53706

The RabA4b GTPase labels a novel, trans-Golgi network compartment displaying a developmentally regulated polar distribution in growing *Arabidopsis thaliana* root hair cells. GTP bound RabA4b selectively recruits the plant phosphatidylinositol 4-OH kinase, PI-4Kβ1, but not members of other PI-4K families. PI-4Kβ1 colocalizes with RabA4b on tip-localized membranes in growing root hairs, and mutant plants in which both the PI-4Kβ1 and -4Kβ2 genes are disrupted display aberrant root hair morphologies. PI-4Kβ1 interacts with RabA4b through a novel homology domain, specific to eukaryotic type IIIβ PI-4Ks, and PI-4Kβ1 also interacts with a $Ca^{2+}$ sensor, AtCBL1, through its $NH_2$ terminus. We propose that RabA4b recruitment of PI-4Kβ1 results in $Ca^{2+}$-dependent generation of PI-4P on this compartment, providing a link between $Ca^{2+}$ and PI-4,5$P_2$–dependent signals during the polarized secretion of cell wall components in tip-growing root hair cells.

## Introduction

In plants, rigid cell walls restrict changes in cell shape and size. As a result, polarized secretion of cell wall components takes on particular importance during growth and development. Polar expansion in root hairs, a polarized plant cell type, is accompanied by accumulation of secretory compartments behind the growing tips of these cells (for reviews see Schnepf, 1986; Dolan, 2001). The *Arabidopsis thaliana* Rab GTPase, RabA4b, specifically labels TGN-like compartments displaying polarized localization in expanding root hair cells (Preuss et al., 2004). Although RabA4b-labeled compartments are thought to deliver new cell wall components to expanding root hair tips, little is known about mechanisms for sorting and targeting secretory vesicles. Rab GTPases regulate membrane trafficking steps by recruiting cytosolic effector proteins to their specific subcellular compartment (for review see Zerial and McBride, 2001; Vernoud et al., 2003). Therefore, to better understand the role RabA4b GTPases play in trafficking secretory cargo, we characterized proteins that selectively interact with RabA4b in its active (GTP bound) conformation.

It is becoming increasingly clear that phosphoinositides play key roles in membrane trafficking steps along the secretory pathway. Specific phosphoinositide isoforms, and proteins that specifically bind these lipids, preferentially mark different subcellular membranes (Thorner, 2001; for reviews see Simonsen et al., 2001; Bankaitis and Morris, 2003). Despite their importance in membrane trafficking, little is known about how their generation and turnover is regulated upon specific elements of the secretory system.

We show that the *A. thaliana* RabA4b GTPase specifically interacts with the phosphatidylinositol 4-OH kinase, PI-4Kβ1, and both colocalize to tip-localized membranes in growing root hairs. In transfer DNA (T-DNA) insertional mutants, where both PI-4Kβ1 and its close relative PI-4Kβ2 are disrupted, root hairs have aberrant morphology. The novel homology (NH) domain, specific to this class of PI-4Ks, is sufficient for interaction with RabA4b, and the $NH_2$-terminal domain of PI-4Kβ1 specifically interacts with *A. thaliana* calcineurin B–like protein (AtCBL1), a $Ca^{2+}$-sensor protein. Finally, tip localization of RabA4b membranes is disrupted by collapsing the tip-focused $Ca^{2+}$ gradient in root hair cells. Based on these observations, we propose a model for RabA4b and PI-4Kβ1 action during polarized root hair expansion.

M.L. Preuss and A.J. Schmitz contributed equally to this paper.
Correspondence to Erik Nielsen: enielsen@danforthcenter.org

Abbreviations used in this paper: AtCBL, *Arabidopsis thaliana* calcineurin B–like proteins; LKU, lipid kinase unique; NH, novel homology; T-DNA, transfer DNA; WT, wild type.

The online version of this article contains supplemental material.

# Results and discussion

Rab GTPases perform their regulatory activities through specific recruitment of cytosolic proteins when the Rab GTPase is in its active (GTP bound) state (for reviews see Novick and Brennwald, 1993; Zerial and McBride, 2001). Therefore, we screened a yeast two-hybrid expression library for interaction with a constitutively active (GTP bound) form of RabA4b. This resulted in identification of a clone containing the COOH-terminal portion of PI-4Kβ1 (PI-4Kβ1Δ1-421), which interacted with the constitutively active (GTP bound) form of RabA4b but not the dominant-negative (GDP bound) form (Fig. 1 A). Further, interaction of PI-4Kβ1Δ1-421 with RabA4b was selective, and no interaction with vacuole-localized RabG3c was detected (Fig. 1 A).

*A. thaliana* contains 12 PI-4Ks in three separate families: PI-4Kα, -β, and -γ (Stevenson et al., 2000; Mueller-Roeber and Pical, 2002). In yeast and animals, these PI-4K families localize to distinct subcellular compartments and have nonredundant functions (Walch-Solimena and Novick, 1999; Hama et al., 2000; Olsen et al., 2003). Consistent with this, we detected no interaction of RabA4b with either PI-4Kα1 or -4Kγ6 (Fig. 1 A). Endosomal Rab GTPases from yeast (Ypt51) and mammals (Rab5) recruit phosphoinositide 3-OH kinases (PI-3Ks), which are necessary for PI-3P accumulation on endosomes (Christoforidis et al., 1999; Gillooly et al., 2003; for review see Zerial and McBride, 2001). AtVPS34, the plant PI-3K, also failed to interact with either active or inactive RabA4b (Fig. 1 A). Collectively, these results suggested that recruitment of PI-4Ks by RabA4b was selective for PI-4Kβ1.

We next determined which PI-4Kβ1 domains were responsible for RabA4b interaction. PI-4Kβ1 contains several domains (Fig. 1 B; Mueller-Roeber and Pical, 2002), including the catalytic domain at the COOH terminus and a lipid kinase unique (LKU) domain that is conserved in type III PI-4Ks of both the α and β families (Balla, 1998; Mueller-Roeber and Pical, 2002). The NH domain is specific to β subfamily members in yeast, animals, and plants (Xue et al., 1999), and a repetitive motif is unique to PI-4Kβ1 and -4Kβ2 in *A. thaliana* (Xue et al., 1999; Mueller-Roeber and Pical, 2002). Testing different combinations of these domains indicated that the NH domain interacted with RabA4b (Fig. 1 C). Surprisingly, in the yeast two-hybrid system, full-length PI-4Kβ1 was not able to interact with RabA4b. This occurred even though the full-length PI-4Kβ1 was expressed at levels similar to the PI-4Kβ1Δ1-421 construct that did interact with RabA4b (unpublished data).

Biochemical methods were used to confirm the RabA4b–PI-4Kβ1 interaction (Fig. 1 D). Affinity columns were generated using *Escherichia coli*–expressed GST-RabA4b, loaded with either GTPγS (active form) or GDP (inactive form). [35S] Met-labeled, in vitro–translated PI-4Kβ1 was passed over the column, and unlike the yeast two-hybrid assay, full-length PI-4Kβ1 was recruited to GST-RabA4b–GTPγS (Fig. 1 D). This indicated that the presence of the NH2 terminus did not abrogate PI-4Kβ1 interaction with RabA4b. The minimal piece necessary for interaction in the yeast two-hybrid system, the NH domain, also associated with the GST-RabA4b–GTPγS
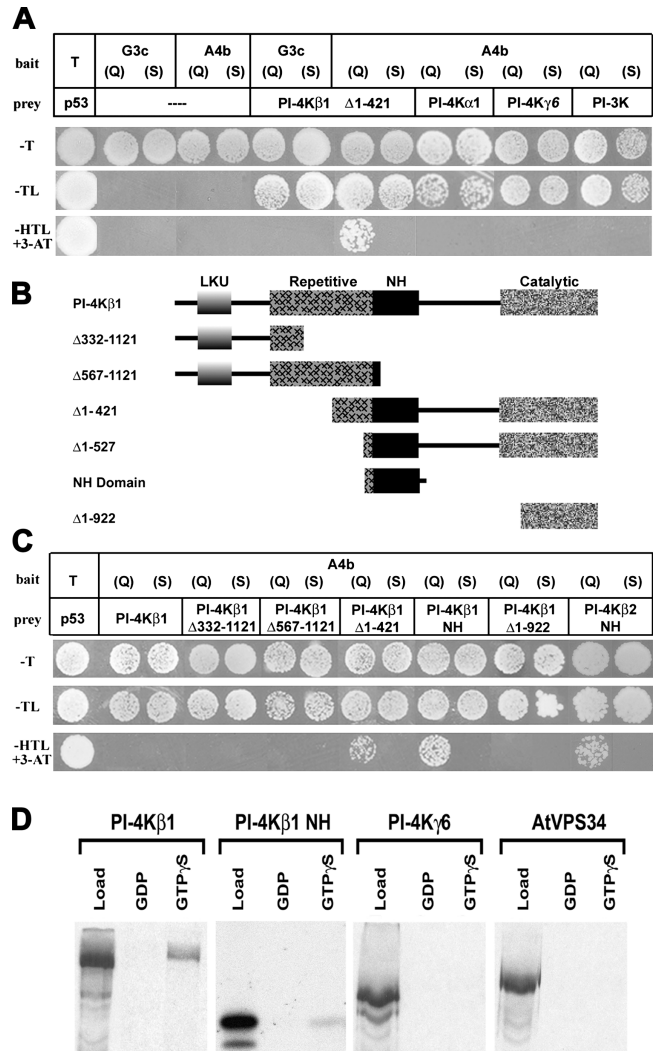


Figure 1. **RabA4b interacts specifically with PI-4Kβ1.** (A) Yeast two-hybrid interaction of PI-4Kβ1Δ1-421 with active GTP bound RabA4b (Q), but not inactive GDP bound RabA4b (S), was detected on high-stringency media (−HisTrpLeu [HTL] + 3-AT). No interaction was observed with vacuolar RabG3c; members of two other plant PI-4K classes, PI-4Kα1 and -4Kγ6; or the plant PI-3K AtVPS34. Presence of prey and/or bait vectors were monitored by growth in absence of tryptophan and leucine (−TL) or tryptophan (−T), respectively. (B) LKU, repetitive, NH, and catalytic domains are indicated. Deletion fragments of PI-4Kβ1 were constructed to determine the binding site of RabA4b. (C) Yeast two-hybrid interaction was seen between active RabA4b (Q) and PI-4Kβ1 fragments containing the NH domain (Δ1-421 and NH) on selective media (−HisTrpLeu + 3-AT). No interaction was observed between RabA4b and other PI-4Kβ1 domains (LKU, repetitive, and catalytic). Surprisingly, full-length PI-4Kβ1 did not interact with RabA4b in the yeast two-hybrid system. (D) PI-4Kβ1 and its NH domain, but not PI-4Kγ6 and AtVPS34, were selectively recruited by active GST-RabA4b–GTPγS, confirming the specificity of the PI-4Kβ1–RabA4b interaction.

at levels similar to the full-length construct. Specificity of the PI-4Kβ1–RabA4b interaction was again demonstrated as PI-4Kγ6 and AtVPS34 were not recruited.

Unlike yeast and mammals, *A. thaliana* has two type IIIβ PI-4Ks. At the protein level, PI-4Kβ2 is 83% identical to PI-4Kβ1. Like PI-4Kβ1, the PI-4Kβ2 NH domain also interacted with the constitutively active form of RabA4b (Fig. 1 C). Therefore, we concluded that both PI-4Kβ1 and -4Kβ2 proteins are
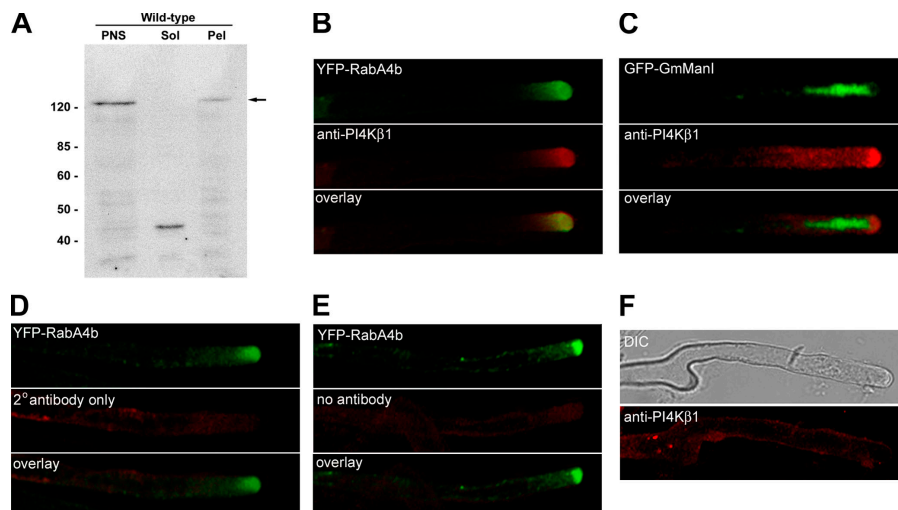
**Figure 2.** **PI-4Kβ1 colocalizes with EYFP-RabA4b on tip-localized compartments in root hair cells.** (A) Anti-PI4Kβ1 recognized an ∼125-kD protein band (arrow) present in postnuclear supernatant (PNS) and membrane fractions (Pel) but not soluble fractions (Sol). The 40-kD band in soluble fractions is present only in green tissues and is not detected in isolated root protein fractions (not depicted). (B–E) *A. thaliana* seedlings were fixed, processed for immunofluorescence, and analyzed by laser confocal microscopy to detect localization of EYFP-RabA4b or EGFP-GmManI fluorescence (green) and PI-4Kβ1 (red). (B) PI-4Kβ1 was tip localized in root hairs. (C) PI-4Kβ1 localization (red) was distinct from Golgi membranes containing EGFP-GmManI (green). (D and E) Detection of tip-localized PI-4Kβ1 compartments was specific, as no tip-localized fluorescence was observed if only anti–PI-4Kβ1 primary antibodies were left out (D) or no antibodies were used (E). (F) Only background fluorescence was observed in root hairs of the PI-4Kβ1/β2 double mutant.

effector proteins that are selectively recruited to the RabA4b GTPase in its active (GTP bound) form.

We next examined the intracellular localization of PI-4Kβ1. EYFP-RabA4b–labeled membranes localize to the tips of growing root hairs (Preuss et al., 2004). Therefore, if PI-4Kβ1 and RabA4b interact in vivo, they should colocalize at the tips of these cells. We generated anti–PI-4Kβ1 antibodies that recognized an endogenous plant protein band of ∼125 kD, the predicted size of PI-4Kβ1 (Fig. 2 A, arrow). PI-4Kβ1 was primarily membrane associated and was not detected in soluble protein fractions from whole plant tissue. Using immunofluorescence and confocal microscopy, we determined that PI-4Kβ1 localized primarily to the tips of root hairs and overlapped with EYFP-RabA4b–labeled compartments (Fig. 2 B). This tip-localized PI-4Kβ1 fluorescence was specific, and no tip-localized fluorescence was detected when anti–PI-4Kβ1 antibodies were left out (Fig. 2, D and E). Further, these EYFP-RabA4b and PI-4Kβ1 membranes were distinct from plant Golgi compartments in these cells, as no significant overlap was observed between PI-4Kβ1 and the plant Golgi marker EGFP-GmManI (Fig. 2 C; Nebenfuhr et al., 1999). These data are consistent with reports from the similar PI-4Ks in yeast and mammals. Direct interaction between mammalian PI4KIIIβ and Rab11 has been reported (de Graaf et al., 2004). Also in yeast, Ypt31 has been shown to interact genetically with Pik1p, although no physical interaction was demonstrated (Sciorra et al., 2004).

We then asked whether PI-4Kβ1 functions in the tip growth of root hair cells. We identified SALK T-DNA insertion lines for both PI-4Kβ1 and -4Kβ2 genes (Fig. 3 A). Plants homozygous for insertions in either the PI-4Kβ1 or -4Kβ2 genes alone showed no obvious phenotype (unpublished data), even though by RT-PCR the appropriate PI-4Kβ transcript was not detected in either insertion line (Fig. 3 B).

Using Western blot (Fig. 3 C) and immunofluorescence (Fig. 2 F), we were not able to detect a functional PI-4Kβ1 protein in the PI-4Kβ1/β2 double mutant. Surprisingly, the highly similar PI-4Kβ2 protein was not recognized by this antibody (see online supplemental material, available at http://www.jcb.org/cgi/content/full/jcb.200508116/DC1). However, based on the lack of PI-4Kβ2 transcript (Fig. 3 B), no PI-4Kβ2 protein should be present. Double-mutant plants were smaller than wild type (WT), and plants homozygous for the PI-4Kβ1 T-DNA insertion but heterozygous for the PI-4Kβ2 T-DNA insertion were intermediate in size (Fig. 3 D). The root hairs of PI-4Kβ1/β2 double mutants were shorter and were abnormal compared with WT root hairs (Fig. 3, E–G). The percentage of aberrant root hairs per root was much higher in PI-4Kβ1/β2 double mutants than in WT plants (Fig. 3 G). This suggested that membrane trafficking required for proper polarized growth is defective in the absence of PI-4Kβ1/β2 activity, and these effects are most pronounced in highly polarized cells, such as the root hair.

Present models suggest that recruitment of PI-4P interacting proteins is essential for sorting and budding of transport vesicles from the Golgi/TGN (Levine and Munro, 2001, 2002). The secretion of cargo from the yeast Golgi complex requires generation of PI-4P by Pik1p (Hama et al., 1999; Walch-Solimena and Novick, 1999). How does lack of PI-4Kβ1/β2 affect the organization of the TGN and the RabA4b compartment? We examined the morphology of TGNs in the PI-4Kβ1/β2 double mutants by electron microscopy. Compared with WT plants (Fig. 4 A, arrows), the TGN in PI-4Kβ1/β2 double mutants showed a lighter staining pattern and clustered budding profiles (Fig. 4, B–D, arrowheads). This phenotype was consistently observed in three independent samples from PI-4Kβ1/β2 double mutants. Over 60% of TGN profiles in PI-4Kβ1/β2 double

**Figure 3.** **PI-4Kβ1/β2 function is essential for normal *A. thaliana* growth and root hair development.** (A) Sequencing of *β1-1* and *β2-1* T-DNA insertion sites confirmed the positions of the T-DNA inserts within PI-4Kβ1 (intron 7) and -4Kβ2 (intron 8) in these two lines. (B) Total RNA was extracted from seedlings homozygous for a T-DNA insertion in PI-4Kβ1 (*β1-1/β1-1*), PI-4Kβ2 (*β2-1/β2-1*), or WT and used for RT-PCR. PI-4Kβ1 transcript was not detected in *β1-1/β1-1*, and PI-4Kβ2 transcript was not detected in *β2-1/β2-1*. Tubulin was amplified as a loading control. (C) Anti–PI-4Kβ1 antibodies detected an ∼125-kD protein band in immunoblots of total protein extracts from WT seedlings but not from PI-4Kβ1/PI-4Kβ2 double-mutant seedlings (*β1-1/β1-1-β2-1/β2-1*). (D) Double mutants (*β1-1/β1-1-β2-1/β2-1*) were smaller than WT plants. Plants homozygous for the PI-4Kβ1 insertion but heterozygous for the PI-4Kβ2 insertion (*β1-1/β1-1/WT/β2-1*) were intermediate in size. (E) Double-mutant root hairs were shorter and growth was disorganized compared with WT. (F) Double-mutant root hairs were classified into six classes based on their phenotype (normal, branched, bulged, popsicle, jagged, and wavy). Representative images of each class are shown. (G, left) WT root hairs were longer than in double mutants. wt, *n* = 817; *β1/β2*, *n* = 797. (right) Percentages of each root hair class were determined in mutant and WT plants. Most WT root hairs were normal in appearance (>90%). However, double mutants had <50% normal root hairs and much higher percentages of each class of deformed root hairs. Root hairs were counted from 19 WT and 21 *β1-1/β1-1/β2-1/β2-1* plants. Error bars indicate SD.
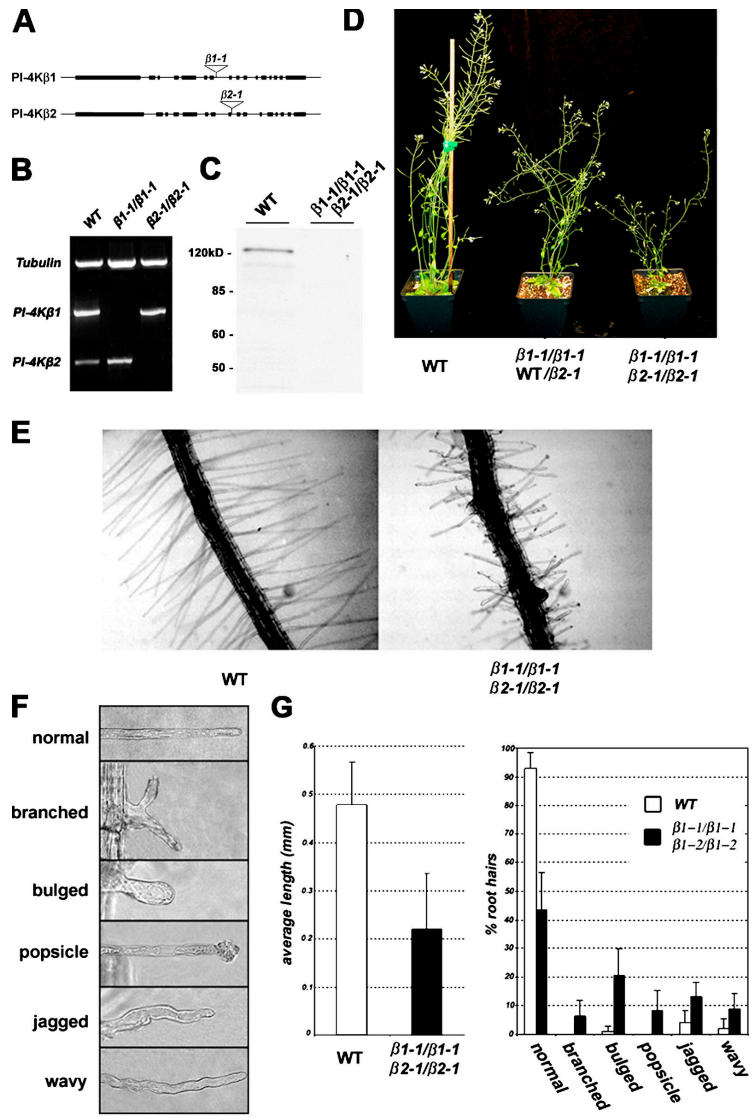


mutants (*n* = 49) displayed this aggregated appearance, which was never observed in WT cells (*n* = 51). Using antibodies specific to RabA4b (Preuss et al., 2004), RabA4b labeled both WT TGN budding profiles (Fig. 4 E, arrows) and the aberrant and aggregated structures in PI-4Kβ1/β2 double mutants (Fig. 4 F, arrowheads). Additionally, even when aggregated structures were not apparent in the double mutant, we observed fewer TGN budding profiles associated with Golgi complexes (Fig. 4 G). Although WT Golgi had a range of budding profiles, the majority of profiles had seven to nine distinct budding profiles per sample. In contrast, the PI-4Kβ1/β2 double mutant usually displayed only one to three budding profiles per sample. Therefore, loss of PI-4Kβ1/β2 function resulted in morphologically altered RabA4b-labeled TGN compartments, consistent with the interference of proper targeting and delivery of cell wall material. From these results, we conclude that PI-4Kβ1/β2 activity is necessary for proper organization of the TGN and post-Golgi secretion.

Finally, we examined the role Ca$^{2+}$ binding proteins play in activation of PI-4Kβ1. Pik1p, the yeast (*Saccharomyces*

*cerevisiae*) orthologue of PI-4Kβ1, is required for vesicular trafficking in the late secretory pathway (Hama et al., 1999; Walch-Solimena and Novick, 1999). Pik1p enzymatic activity is stimulated upon binding of frequenin, an EF-hand–containing Ca$^{2+}$ binding protein (Hendricks et al., 1999; Huttner et al., 2003). Similar Ca$^{2+}$ sensors, AtCBLs, have been described in *A. thaliana* (Kudla et al., 1999). We tested four representative members of this family, AtCBL1, -2, -3, and -5 for interaction with PI-4Kβ1 by yeast two-hybrid analysis (Fig. 5 A). AtCBL1 interacted with the NH$_2$ terminus of PI-4Kβ1. AtCBL2 interaction was also sometimes detected, but growth rates were significantly lower than those of AtCBL1 (unpublished data). The AtCBL1–PI-4Kβ1 interaction was selective, as AtCBL3 and -5 did not interact with PI-4Kβ1. This suggested that the AtCBL1–PI-4Kβ1 interaction is evolutionarily conserved and that AtCBL1, acting as a Ca$^{2+}$ sensor, may modulate PI-4Kβ1 activity.

Proper tip growth in root hair cells requires a tip-focused Ca$^{2+}$ gradient (for review see Dolan, 2001). The interaction between PI-4Kβ1 and AtCBL1 implicates a role for Ca$^{2+}$ in the

regulation of PI-4Kβ1 activity. Therefore, we hypothesized that dissipation of the $Ca^{2+}$ gradient in root hairs would alter the proper localization of EYFP-RabA4b compartments. Treatment of root hairs with A23187, a $Ca^{2+}$ ionophore results in rapid loss of the tip-focused $Ca^{2+}$ gradient (Wymer et al., 1997). When we treated growing root hair cells with A23187, a rapid dispersal of tip-localized EYFP-RabA4b was observed, accompanied by inhibition of root hair growth (Fig. 5, B and C). These results support our hypothesis that localization of RabA4b compartments is dependent on proper recruitment and activation of PI-4Kβ1 activity.

Initiation of tip growth in root hairs and pollen tubes is dependent on the formation of a tip-focused $Ca^{2+}$ gradient (for reviews see Taylor and Hepler, 1997; Dolan, 2001; Yanagisawa et al., 2002). However, it is becoming increasingly clear that lipid-derived signaling molecules play important roles in establishing and maintaining these $Ca^{2+}$ gradients. We have shown that the $NH_2$ terminus of PI-4Kβ1, including the LKU domain, is capable of binding to AtCBL1, a plant homologue of frequenin. In yeast, Pik1p activity is stimulated upon binding of frequenin to the LKU domain in a $Ca^{2+}$-independent manner (Hendricks et al., 1999). But $Ca^{2+}$ does enhance association of frequenin with membranes, which may promote the interaction of frequenin with Pik1p in vivo. If $Ca^{2+}$ binding in the root hair tip stimulates AtCBL1 recruitment to RabA4b membranes, this would ultimately result in increased PI-4P production by PI-4Kβ1 on this compartment.

In summary, the recruitment and activity of PI-4Kβ1 on RabA4b-labeled membranes plays an important role during polarized expansion of root hairs. Previously, we showed that localization of RabA4b-labeled membranes at root hair tips is associated with tip-restricted expansion (Preuss et al., 2004). Our model hypothesizes that recruitment of PI-4Kβ1 and AtCBL1 to RabA4b-labeled membranes results in localized PI-4K activity and enrichment of PI-4P on these compartments. Enrichment of PI-4P may stimulate recruitment of PI-4P binding domain proteins (Levine and Munro, 2002; Godi et al., 2004; Balla et al., 2005), or the PI-4P could be delivered to tip-localized plasma membrane domains via fusion of RabA4b-labeled secretory compartments. There it might be a targeting determinant itself, or plasma membrane–localized PIP-5Ks, recruited to the root hair and pollen tube tips by Rop GTPases (Kost et al., 1999), may phosphorylate PI-4P to PI-4,5P$_2$. This is supported by the observation that PI-4,5P$_2$ is primarily associated with plasma membranes in the tips of root hairs and pollen tubes (Bubb et al., 1998; Kost et al., 1999; Vincent et al., 2005). Therefore, RabA4b-dependent recruitment of PI-4Kβ1 would integrate the perception of tip-focused $Ca^{2+}$ gradients and generation of phosphoinositide-derived signaling molecules for the organization of post-Golgi secretory compartments at the tips of growing root hairs.

## Materials and methods

### Cloning, sequence analysis, and plasmid constructions
Constitutively active (GTP bound) and dominant-negative (GDP bound) forms of RabA4b and -G3c were made using PCR-based techniques and cloned into the pGBKT7 bait vector (CLONTECH Laboratories, Inc.).
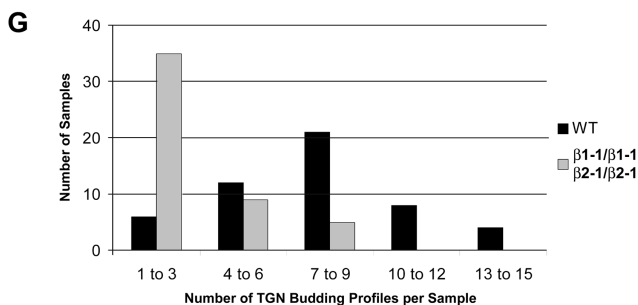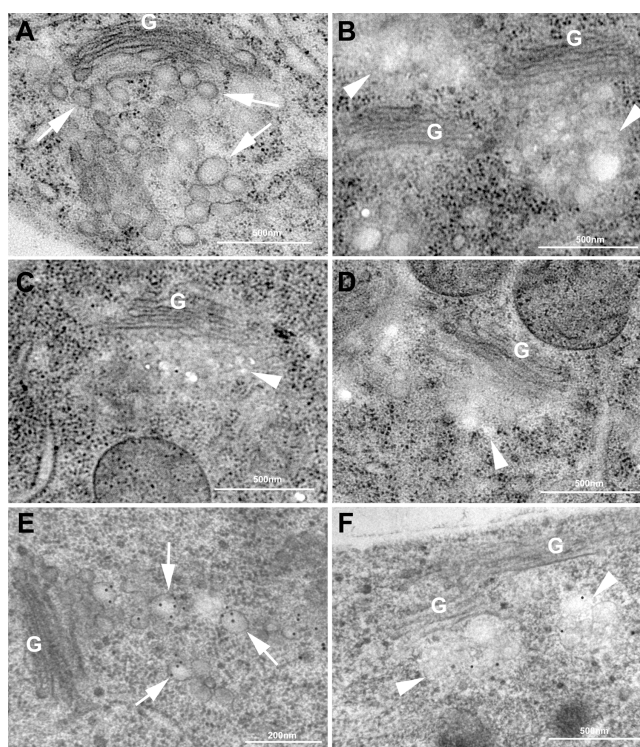


Figure 4. **RabA4b-labeled membranes have altered morphologies in PI-4Kβ1/β2 double mutants.** (A–F) High-pressure frozen/freeze-substituted root tip cells from WT or PI-4Kβ1/β2 double-mutant A. thaliana plants expressing EYFP-RabA4b were processed for EM analysis. (A) Golgi (G) and TGN compartments from WT cells. Note distinct TGN budding profiles (arrows). (B–D) In PI-4Kβ1/β2 double mutants, TGN were often aberrant, with lighter staining and clustered budding profiles (arrowheads). (E and F) Affinity-purified anti-RabA4b antibodies labeled TGN budding profiles in both WT (E, arrows) and PI-4Kβ1/β2 double mutants (F, arrowheads). (G) The numbers of distinct TGN budding profiles associated with each sample (defined as a section containing at least one discernible Golgi stack and associated TGN) were counted. WT averaged seven to nine TGN budding profiles per sample ($n = 51$), whereas only one to three TGN budding profiles were usually observed per sample in double mutants ($n = 49$).

The GTP bound RabA4b mutated Q68→L (primers 5′-TACCGTCTCTCTG-GAACGATACAGAGCCGT-3′ and 5′-TCTCGTCTCTCCAGACCAGCGG-TATCCCAG-3′) and the GDP bound RabA4b mutated S23→N (primers 5′-TGTCGTCTCAAAC-CAACTACTTGCTCGATT-3′ and 5′-AGCACGTCTC-TGGTTTTTCCCAACAGCCGA-3′). Constitutively active and dominant-negative forms of RabG3c were made by mutating Q68→L (primers 5′-TGGGATACTGCAGGGCTAGAGAGGTTCCAAAGT-3′ and 5′-ACT-TTGGAACCTCT-CTAGCCCTGCAGTATCCCA-3′) and T22→N (primers 5′-TGGCGTCTCAAGAA-CTCCTTGATGAATCAG-3′ and 5′-CATCGTCTC-GTTCTTCC-CAACCCCACTGTC-3′), respectively.

Full-length clones from TAIR of PI-3K (C105027), PI-4Kβ1 (U21445), and PI-4Kγ6 (U21028) in the pUNI51 vector were cloned into the pGAD vector for yeast two-hybrid analysis. The PI-4Kα1 sequence in the pFastBac HT vector (a gift from W. Boss, North Carolina

**Figure 5.  The Ca$^{2+}$ sensor AtCBL1 interacts with NH$_2$-terminal domains of PI-4Kβ1.** (A) Yeast two-hybrid interaction between AtCBL1 and the NH$_2$-terminal PI-4Kβ1 fragment (ΔC567-1121; Fig. 1 B) was observed on high-stringency media (−HisTrpLeu [HTL] + 3-AT). (B–D) Disruption of tip-focused Ca$^{2+}$ gradient in root hairs abolished growth and tip-localized EYFP-RabA4b. (B) EYFP-RabA4b fluorescence was visualized in root hairs using time-lapse fluorescence microscopy. Upon treatment with the Ca$^{2+}$ ionophore A23187 (20-min time point), root hair elongation was rapidly inhibited. This correlated with loss of EYFP-RabA4b tip localization and observation of EYFP-RabA4b along the entire root hair (24–30-min time points). When A23187 was washed out, all EYFP-RabA4b fluorescence was lost from the root hair. Neither EYFP-RabA4b tip localization nor root hair tip growth occurred after A23187 washout. The length of the root hair (C) and the percentage of tip fluorescence (D) were measured over time.
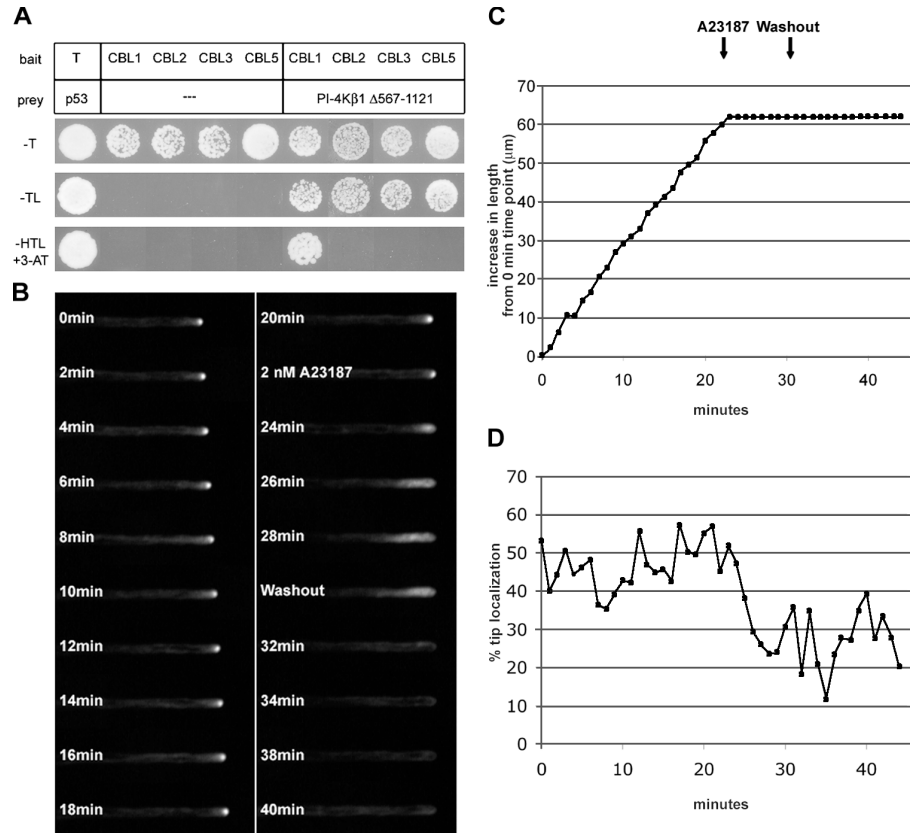


State University, Raleigh, NC; Stevenson-Paulik et al., 2003) was cloned into the pGAD vector. Pieces of PI-4Kβ1 were PCR amplified and cloned into either the pGAD or pGBK vector. The construction of AtCBL1, -2, -3, and -5 in the pAS vectors was described previously (a gift from Y. Guo, National Institute of Biological Sciences, Beijing, China, and J.K. Zhu, University of California, Riverside, Riverside, CA; Guo et al., 2001).

### Yeast two-hybrid screens and interaction assays
The yeast strain AH109 (CLONTECH Laboratories, Inc.) was used for two-hybrid experiments. Using a LiAc transformation protocol (CLONTECH Laboratories, Inc.), the CD4-22 library (Arabidopsis Biological Resource Center; Kim et al., 1997) was screened (∼6 million transformants) and plasmids were rescued from transformants surviving high-stringency selection conditions (−AdeHisLeuTrp + 7.5 mM 3-AT). Plasmids from 127 putative positive yeast colonies were rescued and sequenced. Of these, 30 were tested for the ability to interact with the active or inactive forms of RabA4b, and 4 showed nucleotide specificity in the interaction.

Drop assays were performed by allowing inoculated cultures to grow for 2 d and diluting them to an OD$_{600}$ of 0.02, of which 10 μl drops were spotted on selective and nonselective medium.

### In vitro recruitment assay
RabA4b was PCR cloned into pGEX-6 (GE Healthcare) and transformed into BL21 cells. GST-RabA4b protein was expressed, and active or inactive RabA4b affinity columns were prepared as previously described (Christoforidis and Zerial, 2000). In vitro–translated proteins were generated using a TNT-coupled reticulocyte lysate system (Promega). 45 μl PI-4Kβ1 in vitro–translation product and 150 μl nucleotide stabilization buffer (NS; containing 1 mM GTPγS or GDP) were incubated with 20 μl (18 mg/ml) GST active or inactive RabA4b beads for 2 h at 4°C; washed twice with NS (10 μM nucleotide); washed once with NS (250 mM NaCl and 10 μM nucleotide); washed once with 20 mM Hepes, pH 7.5, 250 mM NaCl, and 1 mM DTT; and eluted with 40 μl elution buffer. 40 μl SB was added to the eluate and boiled for 5 min, and 30 μl was analyzed by SDS-PAGE followed by fluorography. 5% of total in vitro–translation product was also loaded.

### Antibody production
A peptide (CTRQYDYYQRVLNGIL) corresponding to the COOH-terminal AtPI-4Kβ1 sequence was synthesized (Sigma-Aldrich) and used to generate rabbit polyclonal antibodies. Anti-peptide antibodies were affinity purified using the peptide immobilized on Sulfolink beads (Pierce Chemical Co.).

### Protein fractionation
*A. thaliana* seedlings (10–14-d old) were ground in 20 mM Hepes, pH 7.5, 100 mM NaCl, 5 mM MgCl$_2$, 1 mM DTT, 2.5 mM GTP, and protease inhibitors (Roche) and then spun at 2,000 g. The postnuclear supernatant was collected and spun at 100,000 g for 1 h at 4°C. The supernatant (soluble fraction) was separated from the pellet (membrane fraction), and each fraction was analyzed by immunoblotting.

### Immunolocalization of PI-4Kβ1
EYFP-RabA4b (Preuss et al., 2004), EGFP-GmManI (a gift from A. Nebenfuhr, University of Tennessee, Knoxville, TN; Nebenfuhr et al., 1999), and PI-4Kβ1/β2 double-mutant *A. thaliana* seedlings were processed for immunolocalization as described in Preuss et al. (2003) and using a "freeze-shattering" method (Wasteneys et al., 1997). After primary and secondary antibody incubations, slides were mounted with MOVIOL (Calbiochem). Samples were observed on a confocal microscope (LSM 510; Carl Zeiss MicroImaging, Inc.). Z stacks of root hairs were taken and three-dimensional projections from these stacks were used for the final images.

### Characterization of PI-4Kβ1 and -4Kβ2 T-DNA insertion mutants
The PI-4Kβ1 and -4Kβ2 T-DNA insertion mutants were obtained from the SALK T-DNA collection (SALK_040479 and SALK_098069; Arabidopsis Biological Resource Center). Root hairs of WT and mutant plants were imaged using a confocal microscope. The T-DNA insertion site in each line was confirmed by sequencing (primers LBB1 5′-GCGTGGAC-CGCTTGCTGCAACT-3′, B1 5′-TCCAGGCCTTCCTCTCAAAG-3′, and B2 5′-AACCTACCAGGTTGGGACTTG-3′).

### Electron microscopy
*A. thaliana* root tips were loaded in 0.1 M sucrose, frozen in a high-pressure freezer (Baltec HPM 010; Technotrade), and transferred to liquid nitrogen. Substitution was performed in 0.1% uranyl acetate plus

0.2% glutaraldehyde in acetone at −80°C for 72 h and warmed to −50°C for 24 h. After several acetone rinses, samples were infiltrated with Lowicryl HM20 (Electron Microscopy Sciences) for 72 h and polymerized at −50°C under UV light for 72 h. Sections were mounted on formvar-coated nickel grids and blocked for 20 min with 5% (wt/vol) nonfat milk in PBST (0.1% Tween 20). Sections were incubated with primary antibody for 1 h at RT. The sections were rinsed with PBST (0.5% Tween 20) and transferred to the secondary antibody conjugated to 15 nm gold particles for 1 h. Controls were performed by omitting the primary antibody. Sections were stained with 2% uranyl actetate in 70% methanol for 10 min followed by Reynolds's lead citrate (2.6% lead nitrate and 3.5% sodium citrate, pH 12) and observed in a transmission electron microscope (CM120; Philips). Images of TGNs were used for quantification of budding profiles and overall abnormality. Abnormal TGNs were defined as having aggregated budding profiles and a lighter staining pattern.

### Analysis of root hairs with chemical inhibitors
*A. thaliana* seedlings were grown, treated, and analyzed as previously described (Preuss et al., 2004). A23187 (Sigma-Aldrich) was dissolved in DMSO and added at a concentration of 2 nM in 0.25× MS to growing root hairs. Fluorescent signal located within the proximal 15% of the length of the root hair was defined as tip fluorescence, and this was presented as a percentage of the fluorescence detected in the entire root hair.

### Online supplemental material
Fig. S1 shows that purified anti-PI-4Kβ1 antibodies do not recognize PI-4Kβ2. The supplemental text describes how in vitro transcription/translation products of HA-tagged COOH-terminal domains or either PI-4Kβ1 or -4Kβ2 were separated and analyzed to test the specificity of the anti–PI-4Kβ1 antibodies. Online supplemental material is available at http://www.jcb.org/cgi/content/full/jcb.200508116/DC1.

## References

Balla, T. 1998. Phosphatidylinositol 4-kinases. *Biochim. Biophys. Acta.* 1436:69–85.

Balla, A., G. Tuymetova, A. Tsiomenko, P. Varnai, and T. Balla. 2005. A plasma membrane pool of phosphatidylinositol 4-phosphate is generated by phosphatidylinositol 4-kinase type-III alpha: studies with the PH domains of the oxysterol binding protein and FAPP1. *Mol. Biol. Cell.* 16:1282–1295.

Bankaitis, V.A., and A.J. Morris. 2003. Lipids and the exocytotic machinery of eukaryotic cells. *Curr. Opin. Cell Biol.* 15:389–395.

Bubb, M.R., I.C. Baines, and E.D. Korn. 1998. Localization of actobindin, profilin I, profilin II, and phosphatidylinositol-4,5-bisphosphate (PIP2) in *Acanthamoeba castellanii*. *Cell Motil. Cytoskeleton.* 39:134–146.

Christoforidis, S., and M. Zerial. 2000. Purification and identification of novel Rab effectors using affinity chromatography. *Methods.* 20:403–410.

Christoforidis, S., M. Miaczynska, K. Ashman, M. Wilm, L. Zhao, S.C. Yip, M.D. Waterfield, J.M. Backer, and M. Zerial. 1999. Phosphatidylinositol-3-OH kinases are Rab5 effectors. *Nat. Cell Biol.* 1:249–252.

de Graaf, P., W.T. Zwart, R.A.J. van Dijken, M. Deneka, T.K.F. Schulz, N. Geijsen, P.J. Coffer, B.M. Gadella, A.J. Verkleij, P. van der Sluijs, and P.M.P. van Bergen en Henegouwen. 2004. Phosphatidylinositol 4-kinaseβ is critical for functional association of rab11 with the Golgi complex. *Mol. Biol. Cell.* 15:2038–2047.

Dolan, L. 2001. How and where to build a root hair. *Curr. Opin. Plant Biol.* 4:550–554.

Gillooly, D.J., C. Raiborg, and H. Stenmark. 2003. Phosphatidylinositol 3-phosphate is found in microdomains of early endosomes. *Histochem. Cell Biol.* 120:445–453.

Godi, A., A. Di Campli, A. Konstantakopoulos, G. Di Tullio, D.R. Alessi, G.S. Kular, T. Daniele, P. Marra, J.M. Lucocq, and M.A. De Matteis. 2004. FAPPs control Golgi-to-cell-surface membrane traffic by binding to ARF and PtdIns(4)P. *Nat. Cell Biol.* 6:393–404.

Guo, Y., U. Halfter, M. Ishitani, and J.K. Zhu. 2001. Molecular characterization of functional domains in the protein kinase SOS2 that is required for plant salt tolerance. *Plant Cell.* 13:1383–1400.

Hama, H., E.A. Schnieders, J. Thorner, J.Y. Takemoto, and D.B. DeWald. 1999. Direct involvement of phosphatidylinositol 4-phosphate in secretion in the yeast *Saccharomyces cerevisiae*. *J. Biol. Chem.* 274:34294–34300.

Hama, H., J.Y. Takemoto, and D.B. DeWald. 2000. Analysis of phosphoinositides in protein trafficking. *Methods.* 20:465–473.

Hendricks, K.B., B.Q. Wang, E.A. Schnieders, and J. Thorner. 1999. Yeast homologue of neuronal frequenin is a regulator of phosphatidylinositol-4-OH kinase. *Nat. Cell Biol.* 1:234–241.

Huttner, I.G., T. Strahl, M. Osawa, D.S. King, J.B. Ames, and J. Thorner. 2003. Molecular interactions of yeast frequenin (Frq1) with the phosphatidylinositol 4-kinase isoform, Pik1. *J. Biol. Chem.* 278:4862–4874.

Kim, J., K. Harter, and A. Theologis. 1997. Protein-protein interactions among the Aux/IAA proteins. *Proc. Natl. Acad. Sci. USA.* 94:11786–11791.

Kost, B., E. Lemichez, P. Spielhofer, Y. Hong, K. Tolias, C. Carpenter, and N.H. Chua. 1999. Rac homologues and compartmentalized phosphatidylinositol 4, 5-bisphosphate act in a common pathway to regulate polar pollen tube growth. *J. Cell Biol.* 145:317–330.

Kudla, J., Q. Xu, K. Harter, W. Gruissem, and S. Luan. 1999. Genes for calcineurin B-like proteins in *Arabidopsis* are differentially regulated by stress signals. *Proc. Natl. Acad. Sci. USA.* 96:4718–4723.

Levine, T.P., and S. Munro. 2001. Dual targeting of Osh1p, a yeast homologue of oxysterol-binding protein, to both the Golgi and the nucleus-vacuole junction. *Mol. Biol. Cell.* 12:1633–1644.

Levine, T.P., and S. Munro. 2002. Targeting of Golgi-specific pleckstrin homology domains involves both PtdIns-4-kinase-dependent and -independent components. *Curr. Biol.* 12:695–704.

Mueller-Roeber, B., and C. Pical. 2002. Inositol phospholipid metabolism in *Arabidopsis*. Characterized and putative isoforms of inositol phospholipid kinase and phosphoinositide-specific phospholipase C. *Plant Physiol.* 130:22–46.

Nebenfuhr, A., L.A. Gallagher, T.G. Dunahay, J.A. Frohlick, A.M. Mazurkiewicz, J.B. Meehl, and L.A. Staehelin. 1999. Stop-and-go movements of plant Golgi stacks are mediated by the acto-myosin system. *Plant Physiol.* 121:1127–1142.

Novick, P., and P. Brennwald. 1993. Friends and family: the role of the Rab GTPases in vesicular traffic. *Cell.* 75:597–601.

Olsen, H.L., M. Hoy, W. Zhang, A.M. Bertorello, K. Bokvist, K. Capito, A.M. Efanov, B. Meister, P. Thams, S.N. Yang, et al. 2003. Phosphatidylinositol 4-kinase serves as a metabolic sensor and regulates priming of secretory granules in pancreatic beta cells. *Proc. Natl. Acad. Sci. USA.* 100:5187–5192.

Preuss, M.L., D.P. Delmer, and B. Liu. 2003. The cotton kinesin-like calmodulin-binding protein associates with cortical microtubules in cotton fibers. *Plant Physiol.* 132:154–160.

Preuss, M.L., J. Santos-Serna, T.G. Falbel, S.Y. Bednarek, and E. Nielsen. 2004. The *Arabidopsis* Rab GTPase RabA4b localizes to the tips of growing root hair cells. *Plant Cell.* 16:1589–1603.

Schnepf, E. 1986. Cellular polarity. *Annu. Rev. Plant Physiol.* 37:23–47.

Sciorra, V.A., A. Audhya, A.B. Parsons, N. Segev, C. Boone, and S.D. Emr. 2004. Synthetic genetic array analysis of the PtdIns 4-kinase Pik1p identifies components in a Golgi-specific Ypt31/rab-GTPase signaling pathway. *Mol. Biol. Cell.* 16:776–793.

Simonsen, A., A.E. Wurmser, S.D. Emr, and H. Stenmark. 2001. The role of phosphoinositides in membrane transport. *Curr. Opin. Cell Biol.* 13:485–492.

Stevenson, J.M., I.Y. Perera, I.I. Heilmann, S. Persson, and W.F. Boss. 2000. Inositol signaling and plant growth. *Trends Plant Sci.* 5:357.

Stevenson-Paulik, J., J. Love, and W.F. Boss. 2003. Differential regulation of two *Arabidopsis* type III phosphatidylinositol 4-kinase isoforms. A regulatory role for the pleckstrin homology domain. *Plant Physiol.* 132:1053–1064.

Taylor, L.P., and P.K. Hepler. 1997. Pollen germination and tube growth. *Annu. Rev. Plant Physiol. Plant Mol. Biol.* 48:461–491.

Thorner, J.W. 2001. Greasing the wheels of secretory transport. *Nat. Cell Biol.* 3:E196–E198.

Vernoud, V., A.C. Horton, Z. Yang, and E. Nielsen. 2003. Analysis of the small GTPase gene superfamily of *Arabidopsis*. *Plant Physiol.* 131:1191–1208.

Vincent, P., M. Chua, F. Nogue, A. Fairbrother, H. Mekeel, Y. Xu, N. Allen, T.N. Bibikova, S. Gilroy, and V.A. Bankaitis. 2005. A Sec14p-nodulin domain

phosphatidylinositol transfer protein polarizes membrane growth of *Arabidopsis thaliana* root hairs. *J. Cell Biol.* 168:801–812.

Walch-Solimena, C., and P. Novick. 1999. The yeast phosphatidylinositol-4-OH kinase pik1 regulates secretion at the Golgi. *Nat. Cell Biol.* 1:523–525.

Wasteneys, G.O., J. Willingale-Theune, and D. Menzel. 1997. Freeze shattering: a simple and effective method for permeabilizing higher plant cell walls. *J. Microsc.* 188:51–61.

Wymer, C.L., T.N. Bibikova, and S. Gilroy. 1997. Cytoplasmic free calcium distributions during the development of root hairs of *Arabidopsis thaliana*. *Plant J.* 12:427–439.

Xue, H.W., C. Pical, C. Brearley, S. Elge, and B. Muller-Rober. 1999. A plant 126-kDa phosphatidylinositol 4-kinase with a novel repeat structure. Cloning and functional expression in baculovirus-infected insect cells. *J. Biol. Chem.* 274:5738–5745.

Yanagisawa, L.L., J. Marchena, Z. Xie, X. Li, P.P. Poon, R.A. Singer, G.C. Johnston, P.A. Randazzo, and V.A. Bankaitis. 2002. Activity of specific lipid-regulated ADP ribosylation factor-GTPase–activating proteins is required for Sec14p-dependent Golgi secretory function in yeast. *Mol. Biol. Cell.* 13:2193–2206.

Zerial, M., and H. McBride. 2001. Rab proteins as membrane organizers. *Nat. Rev. Mol. Cell Biol.* 2:107–117.